J Anesth (2015) 29:379–385
DOI 10.1007/s00540-014-1929-0

ORIGINAL ARTICLE

Modeling of safe window for percutaneous thoracic sympathectomy

Do Won Lee · Jung Min Hong · Boo Young Hwang · Tae Kyun Kim · Eun Soo Kim

Received: 15 July 2014 / Accepted: 26 September 2014 / Published online: 10 October 2014

Abstract
Purpose Despite the many benefits of percutaneous thoracic sympathectomy, it also has serious complications such as pneumothorax. This study was conducted in order to determine the safe percutaneous entering window and angles for the needle during T2 and T3 thoracic sympathectomy avoiding pneumothorax.
Methods Transverse section of CT images that crosses at the middle of the T2 or T3 vertebral body was selected. Medial and lateral imaginary lines were drawn from the dorsoventrally midpoint on the lateral surface of the vertebral body (v) to the skin. The medial one was drawn to the skin medially as much as possible tangent to the vertebral body (vM). The lateral one was drawn to the skin tangent to parietal pleura (vL). c was defined as the point where the midsagittal line meets the skin. The distance cM and cL, the angle aM and aL made between the midsagittal line and vM or vL lines were measured. To determine the relations between patients' covariates and measured data, mixed-effect population analysis was performed for the cL, aL, and vL.
Results In males, the mean values of cL were 85.3 and 79.2 mm for T2 and T3, respectively. In females, they were 71.5 and 63.7 mm for T2 and T3, respectively. Population analysis revealed that cL was best described with age, weight, gender covariates, and interindividual variability. The aL was best described with BMI and gender covariates.
Conclusions The covariates' relationship and interindividual variability resulting from the mixed-effect analysis enhanced individual prediction for safe widows.

Keywords Percutaneous thoracic sympathectomy · Pneumothorax · Mixed-effect modeling · Interindividual variability

Introduction

Although the effect of percutaneous thoracic sympathectomy (PTS) on hyperhidrosis, angina, and complex regional pain syndromes (CRPS) is unfortunately controversial and has limited evidences [1, 2], PTS has been widely applied to patients who suffered from vascular occlusion, Raynaud's syndrome, hyperhidrosis, CRPS, and Prinzmetal's angina since its introduction by Wilkinson [3]. Although its efficacy has long been debated for its recurrence, the improved results and its technique have guaranteed the benefit and efficacies of this procedure throughout many years of evolution [4–8]. In addition, PTS could be performed on out patients with just a light sedation or local analgesic infiltration and the results can be assessed immediately after the procedure.

Despite the many benefits of percutaneous thoracic sympathectomy, there are also several complications, including pneumothorax, intercostal neuralgia, excessive dryness or compensatory hyperhidrosis, and superficial wound infection [1, 4, 7–9]. Most of all, the life-threatening pneumothorax might be a serious complication that every physician wants to avoid. The incidence of pneumothorax after percutaneous thoracic sympathectomy has

D. W. Lee · J. M. Hong · B. Y. Hwang · T. K. Kim · E. S. Kim
Department of Anesthesia and Pain Medicine, School of Medicine, Pusan National University, Busan, Korea

D. W. Lee · J. M. Hong · B. Y. Hwang · T. K. Kim (✉) · E. S. Kim
Biomedical Research Institute, Pusan National University Hospital, 179 Gudeok-ro, Seo-gu, Busan 602-739, Korea
e-mail: anesktk@pusan.ac.kr

been reported as 0.2–0.9 %, varying between reports [4, 7–9]. Despite what appears to be very low incidence, once pneumothorax occurs, it must be regarded as a serious life-threatening condition. Conventional tomography or fluoroscopic cone-beam CT was recently introduced in order to provide guidance for interventions with high resolution in 3D [5, 7]. However, there is no evidence indicating that they could reduce the incidence of pneumothorax more than cases in which a conventional c-arm was used.

Careful alignment of the needle trajectory around osseous structures in the spine and keeping a distance from the pleura is required to avoid a pneumothorax. Two key elements of needle placement include location of percutaneous insertion and needle angle in relation to the skin. Approaches that are too lateral to the midline increase the risk of pneumothorax and approaches that are too close to the midline increase the risk of inability to reach the needle to the appropriate depth because the trajectory passes through bony structures.

The aim of this study is identifying the appropriate percutaneous window and needle angle to avoid penetrating the pleura. The optimal needle placement and trajectory angle would be so variable from person to person that the trajectory prediction demands explanation of interindividual variability. This study was investigated by the means of mixed-effect population modeling to optimize prediction of needle placement and trajectory angle.

Methods

CT images of patients aged 20–70 years were investigated from the database of the hospital patients' information center after approval of the Institutional Review Board. CT images were selected among patients who had no pathologic disease such as lung parenchymal or pleural disease and musculoskeletal abnormalities. Patients who had metabolic diseases or any other diseases that could result in body deformity were also excluded.

Transverse sections from CT scan at T2 and T3 were reviewed and selected. A transverse section that crosses at the middle of the T2 or T3 vertebral body was selected. If the section crosses the rib head, the next section just below the rib head was selected for analysis. Figure 1 shows the method of measurement. Medial and lateral imaginary lines were drawn from the dorsoventral midpoint of the lateral surface of vertebral body (v) to the skin. Sympathetic ganglion is supposed to be located at v. The medial one was drawn from the v to the skin medially as much as possible tangent to the vertebral body (vM). The lateral one was also drawn from v to the skin tangent to the parietal pleura (vL). The line that crosses the center of the vertebral body dorsoventrally was defined as the midsagittal line. c

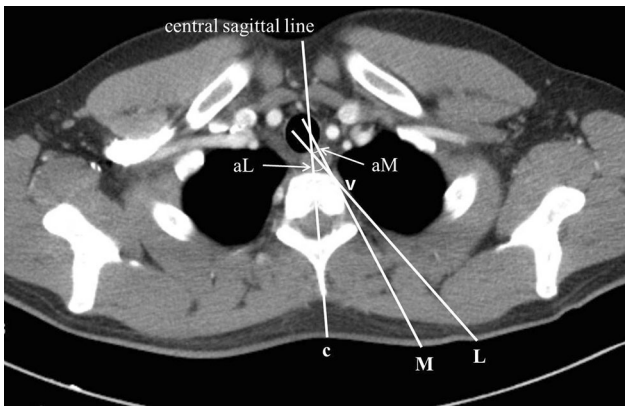

Fig. 1 Schematic drawing shows medial (vM) and lateral (vL) limit trajectory and safe entering window (between M and L) for percutaneous thoracic sympathectomy. The aM and aL are the angles that are made between the central sagittal line and extension of vM or vL

was defined as the point where the midsagittal line meets the skin. The distance between c and M (cM), c and L (cL) was measured and difference between cL and cM was calculated (ML). The M indicates the most medial point for insertion of the needle so that it is able to reach the target point (v) without obstacles such as articular process or vertebral body itself. Point L means the maximum lateral point through which a needle can be inserted with avoiding pneumothorax. Beyond point L, the needle cannot reach the point v without passing through the radiolucent part of the CT image, which means the lung. The ML means the length of the window for needle insertion. The angle aM and aL, which were made between the midsagittal lines and vM or vL lines, were measured. The depths defined as distance from v to M (vM), from v to L (vL) were measured.

Data were reported as the mean ± SD and analyzed using repeated measures of analysis of variance (RMANOVA). The data were introduced into version 17.0 of the statistical package SPSS for Windows (SPSS Inc., Chicago, IL, USA) for subsequent analysis. To determine relations between patients' covariates and measured data, multiple linear mixed-effect analysis was performed on the cL, aL, and vL using NONMEM® (version 7.2, Icon Development Solutions, Ellicott City, MD, USA) [10]. NONMEM® is one of the statistical tests, which stands for 'nonlinear mixed-effect modeling'. At the same time, NONMEM is a kind of modeling tool that has been known as a powerful tool for mixed-effect (fixed and random effects) modeling. This kind of technique could precisely identify not only coefficients of covariates (fixed effect) but also interindividual and intra-individual variability (random effect) as well.

An additive variance model was used to describe the interindividual variability (IIV) of the measurement

parameters cL, aL, and vL at each thoracic level according to the following equation:

$$\theta_j = \theta_{TV} + \eta_j \quad (1)$$

where θ_{TV} is a population mean value for the measurement parameters of the population, θ_j is the individual post hoc estimate for the parameter in the jth subject and η_j is a random variable representing the interindividual variability between individual (θ_j) and population (θ_{TV}) values, which is a normally distributed random variable with a mean of zero and a variance ω^2. The interindividual variability was assumed to be equal for both vertebral levels.

To describe the residual errors, additive error models was modeled using the following equation:

$$M_{ij} = M_{pred,ij} + \varepsilon_{ij} \quad (2)$$

where M_{ij} is the ith level observed measurement in the jth subject; $M_{pred,ij}$ is the ith level predicted measurement based on the study parameters in the jth patient; and ε_{ij} are additive error terms, respectively, which are normally distributed random variables with a mean of 0 and variance of σ^2.

The potential covariates affecting parameters were explored for age, body weight, height, and BMI. The minimal value of the NONMEM objective function (equal to minus twice the log likelihood, $-2\Delta LL$) was used as a test for statistical significance of the additional covariate effects. An addition of a parameter was determined by a p value of less than 0.05, representing a decrease in objective function value of at least 3.84 points (χ^2 distribution, degrees of freedom = 1). The models were also evaluated using graphical methods, which was facilitated by use of xpose4 [version 4.0 on the R statistical software package (version 2.13.1, the R Foundation for Statistical Computing, Vienna, Austria)] [11].

For each measurement, the prediction error (PE) was calculated as follows:

$$PE\,(\%) = \left[\frac{M_o - M_p}{M_p}\right] \times 100$$

where M_p is the predicted measurement and M_o is the observed measurement. Subsequently, the median prediction error (MDPE) and median absolute prediction error (MDAPE), which indicate bias and inaccuracy, respectively, were calculated in order to examine the quality of the prediction of the models for the population.

$$MDPE\,(\%) = \text{median}\{PE\}$$

$$MDAPE\,(\%) = \text{median}\{|PE|\}$$

Predictive performance was assessed in terms of pooled bias and inaccuracy by determination of the MDPE and MDAPE over all measurement. MDPE and MDAPE were calculated with population prediction. When the 95 % confidence interval of the pooled MDPE included zero, it was concluded that the bias was not significant.

Table 1 Demographic data

	Males ($n = 47$)	Females ($n = 53$)
Age (years)	45.2 (12.8)	46.6 (11.7)
Height (cm)	171.5 (6.1)	158.8 (6)[a]
Weight (kg)	70.8 (9.7)	57.2 (7.4)[a]
BMI	24.0 (2.9)	22.7 (2.9)[a]

[a] $p < 0.05$ compared to males

For the final models, for evaluation of the accuracy and robustness, a non-parametric bootstrap analysis was performed as an internal model validation. Re-sampling of the dataset and bootstrap replicates was generated 1,000 times from the original data set with replacement. The ideal method for validation of the model is prospective testing, which is known as external validation. However, internal validation is an alternative to the external validation and the bootstrap is one of the recommended methods for internal validation [12, 13].

From the result of the model, simulation was performed with various patients, including obese and lean, young and old age, and males and females in order to demonstrate the variable safe margin of the thoracic sympathectomy trajectory.

External validation for trajectory was performed with another subset of thoracic CT images. It was conducted by means of drawing a predicted PTS trajectory line to the target and determining whether the predicted trajectory for PTS penetrate the lung or not.

Results

One hundred transverse sections of CT scan were investigated at each T2 and T3 level. Average age, weight, height, BMI, and gender were 46 (12.2) year, 63.6 (10.9) kg, 164.8 (8.7) cm, 23.3 (3) m/kg^2, and 47/53 (M/F), respectively. Patients' demographics and measured data presented according to gender and thoracic levels are shown in Table 1. Gender differences were observed for weight, height, and BMI.

In Fig. 1, the safety window starts from point M to point L. With regard to males, the safety window spans from 35.8 mm (cM) to 85.3 mm (cL) for T2 level and from 32.5 mm (cM) to 79.2 mm (cL) for T3 level. As a result, the window widths for males are 49.4 and 46.7 mm for T2 and T3 levels, respectively. In females, the safety window spans from 34.7 mm (cM) to 71.5 mm (cL) for T2 level and from 30.2 mm (cM) to 63.7 mm (cL) for T3 level. As a

Table 2 Measured data according to levels and sexual differences

Level	Males ($n = 47$)		Females ($n = 53$)	
	2	3	2	3
cM (mm)	35.8 (6.2)	32.5 (5.5)[b]	34.7 (7.3)	30.2 (5.2)[a,b]
cL (mm)	85.3 (14.2)	79.2 (12.2)[b]	71.5 (13.4)[a]	63.7 (11.9)[a,b]
ML (mm)	49.4 (12.9)	46.7 (12.1)	36.8 (10.9)[a]	33.5 (10.3)[a]
aM (°)	12.6 (3.8)	12.7 (3.7)	14.8 (4.8)[a]	13.1 (3)[b]
aL (°)	37.7 (5.9)	37.8 (5.4)	35.9 (5.7)	33.8 (4.8)[a,b]
aML (°)	25.1 (5.3)	25.1 (5.4)	21.1 (4.9)[a]	20.7 (4.8)[a]
vM (mm)	89.5 (8.5)	84.2 (8)[b]	79.8 (10.6)[a]	75.9 (9)[a,b]
vL (mm)	112.8 (11.3)	105.1 (10.6)[b]	98 (12.7)[a]	90.5 (11.8)[a,b]

Data are shown as mean (SD)

BMI body mass index [weight (kg)/height (m^2)], *cM* medial limit of safe window, *cL* lateral limit of safe window, *ML* safe window width, *aM* angle that is made between central sagittal line and medial limit trajectory line, *aL* angle that is made between central sagittal line and lateral limit trajectory line, *aML* angle that is made between medial and lateral limit trajectory line, *vM and vL* depth of medial and lateral limit trajectory

[a] $p < 0.05$ compared to males

[b] $p < 0.05$ compared to thoracic level 2

result, the window widths for females are 36.8 and 33.5 mm for T2 and T3 levels, respectively (Table 2).

For the length of cL and cM, differences were observed between thoracic levels. The cL of T2 thoracic level was longer than that of T3. The cL showed gender differences as well; the length of the males was longer. For the angles aM, aL, and aML, in general, differences were observed between gender. The aL and aML of males were wider, however, the aM of females was wider. No difference of angle measurements (aM, aL, and aML) was observed between thoracic levels. For depth, vM and vL showed gender difference and all measurements for males were longer than those for females. The vM and vL of T2 thoracic level was longer than that of T3.

A summary of the results of the final models is shown in Table 3.

For the results of modeling, the model of cL was best described with age, weight, and gender covariate. Weight and age were incorporated linearly by being centered with each median values.

Population cL measurements of T2 and T3 could be described as follows:

$$73.4\ (66.4 \text{ for T3}) + 0.615 \times (\text{weight} - 60.5) + 0.355 \times (\text{age} - 47.5) + 6.79\ (0 \textit{ for female})$$

The model of aL was best described with gender and BMI covariate. Population aL measurements of T2 and T3 could be described as follows:

$$35.6\ (34.6 \text{ for T3}) + 0.714 \times (\text{BMI} - 23.1) + 1.94\ (0 \text{ for female})$$

The model of vL was best described with weight, age and gender covariate. Population vL measurements of T2 and T3 could be described as follows:

$$100\ (92.9 \text{ for T3}) + 0.643 \times (\text{weight} - 60.5) + 0.345 \times (\text{age} - 47.5) + 6.51\ (0 \text{ for female})$$

Table 3 shows results estimates and its standard error comparing with the median and confidence interval of bootstrapping results. Plots of individual predicted values versus measured values showed close correlations in Fig. 2.

Table 3 Population parameter estimates, inter-individual variability and median parameter values of the nonparametric bootstrap replicates of the final model

Model	cL		aL		vL	
	Coefficient (RSE, %)	Bootstrap results (median, CI)	Coefficient (RSE, %)	Bootstrap results (median, CI)	Coefficient (RSE, %)	Bootstrap results (median, CI)
Fixed effects						
Intercept (T2)	73.4 (2.1)	73.4 (70.2, 76.4)	35.6 (1.8)	35.6 (34.3, 36.9)	100 (1.4)	100.4 (97.6, 103.3)
Intercept (T3)	66.4 (2.1)	66.5 (63.6, 69.2)	34.6 (1.6)	34.6 (33.4, 35.7)	92.9 (1.4)	92.8 (90.1, 95.5)
Weight	0.615 (20.5)	0.614 (0.354, 0.854)			0.643 (17.4)	0.639 (0.407, 0.862)
Age	0.355 (21.9)	0.355 (0.206, 0.496)			0.345 (20.1)	0.346 (0.202, 0.473)
BMI			0.714 (21.7)	0.723 (0.388, 1.01)		
Sex	6.79 (41.4)	6.86 (1.67, 12.95)	1.93 (45.5)	1.95 (0.159, 3.73)	6.51 (39.2)	6.58 (1.58, 11.7)
	Variance (RSE, %)		Variance (RSE, %)		Variance (RSE, %)	
Random effects						
IIV (ω)	9.4 (44.2)		4 (43.6)		8.7 (42.9)	
Residual (σ)	5.6 (38.5)		3 (36.7)		3.5 (37.8)	

RSE relative standard error, *CI* confidence interval, *IIV* interindividual variability

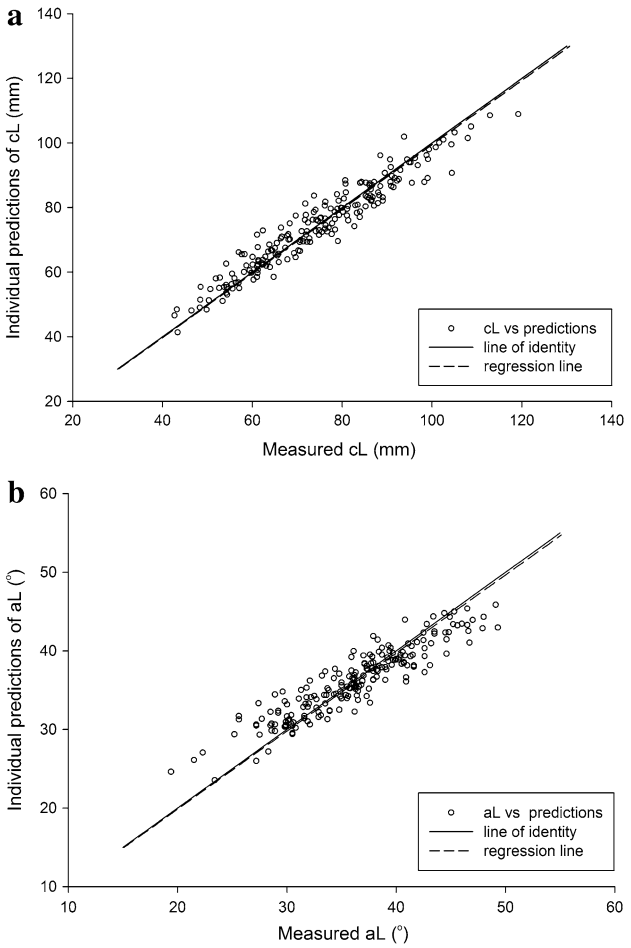

Fig. 2 Plot shows predicted versus the measured cL (**a**) or aL (**b**)

Bias and inaccuracy represented with MDPE and MDAPE are shown in Table 4. Bias of the cL, aL, and vL are 0.5, 0 and 0.2 (%), respectively. Confidence intervals of all bias include 0, so that it can be said that there was no bias for the estimates. The inaccuracy of the cL, aL, and vL estimates are 11.5, 10.5, and 7.3 (%), respectively.

Simulation was done for variable age, weight, and BMI for each gender. Results of the simulation for cL, aL, and vL are drawn in a schematic plot in Fig. 3. With heavier the weight and older age, the cL length becomes longer.

Another subset of 36 patients of T2 and T3 CT scan were involved for external validation of the model. Demographic characteristics of external validation population were not different from the population that used for modeling. Mean ± SD of age, weight, height, BMI and gender are 46.6 ± 11.1 year, 63.6 ± 11.9 kg, 165.6 ± 9.1 cm, 23.1 ± 3.2 kg/m^2 and M/F (17/19), respectively.

External validation for trajectory was not started from the L point but the entering point was shifted medially to take into account the interindividual variability. A medially shifted point from the predicted L point as much as one-tailed 0.5 and 2.5 % point of normal distribution of inter-individual variability was determined as the appropriate point for evaluating the chances of pneumothorax. As a result, the shifting distance for validation would be located at 18.4 or 24.3 mm medial from the predicted L point. When point L was shifted 24.3 mm medially, there was no case of trajectory that penetrates the lung. If 18.4 mm is taken for the medial shift, the validation would result in one level out of 72 levels (36 patients) penetrating the lung, which means the incidence reaches as high as 1.4 %.

Table 4 Prediction performance

	cL	aL	vL
MDPE (%)	0.5	0	0.02
(95 % CI)	(−0.5, 1.5)	(−1.2, 1.1)	(−0.46, 0.49)
MDAPE (%)	11.5	10.5	7.3
(95 % CI)	(10.7, 12.4)	(9.6, 11.5)	(6.9, 7.8)

MDPE median prediction error, *MDAPE* median absolute prediction error

Discussion

This study was conducted in order to determine a safe entry zone and appropriate angle for a percutaneous thoracic sympathectomy avoiding pneumothorax. The entry point for avoidance of pneumothorax in males should not be beyond the distance of 85.3 and 79.2 mm from the midline of the back for T2 and T3, respectively. In females, it was 71.5 and 63.7 mm for T2 and T3, respectively. However, those numbers were calculated from the statistically simple means. One of the purposes of modeling in this study would be suggesting some safety guidelines for PTS. From the viewpoint of that purpose, it is necessary to suggest some safety limits rather than listing a simple population mean. Many of the measurements must be influenced by individual characteristics, such as weight, height, age, BMI, etc. The modeling process could help us to solve those individual influences on several measurements.

MDPE or MDAPE used for model validation showed good results so that the model has appropriate accuracy and no bias. However, no bias and accuracy does not mean that the measurements of cL or aL themselves are the safe entering point or angle. If the model fits the data well, the predicted values should be normally distributed around the population mean. This means that, theoretically, half of the predicted cL has a chance of pneumothorax due to inter-individual variability and measurement error. Therefore, recommended entry point should be more medial side than the predicted L point. Medially shifted point from predicted cL as much as one tailed 0.5 % point of normal distribution of interindividual variability (24.3 mm) would

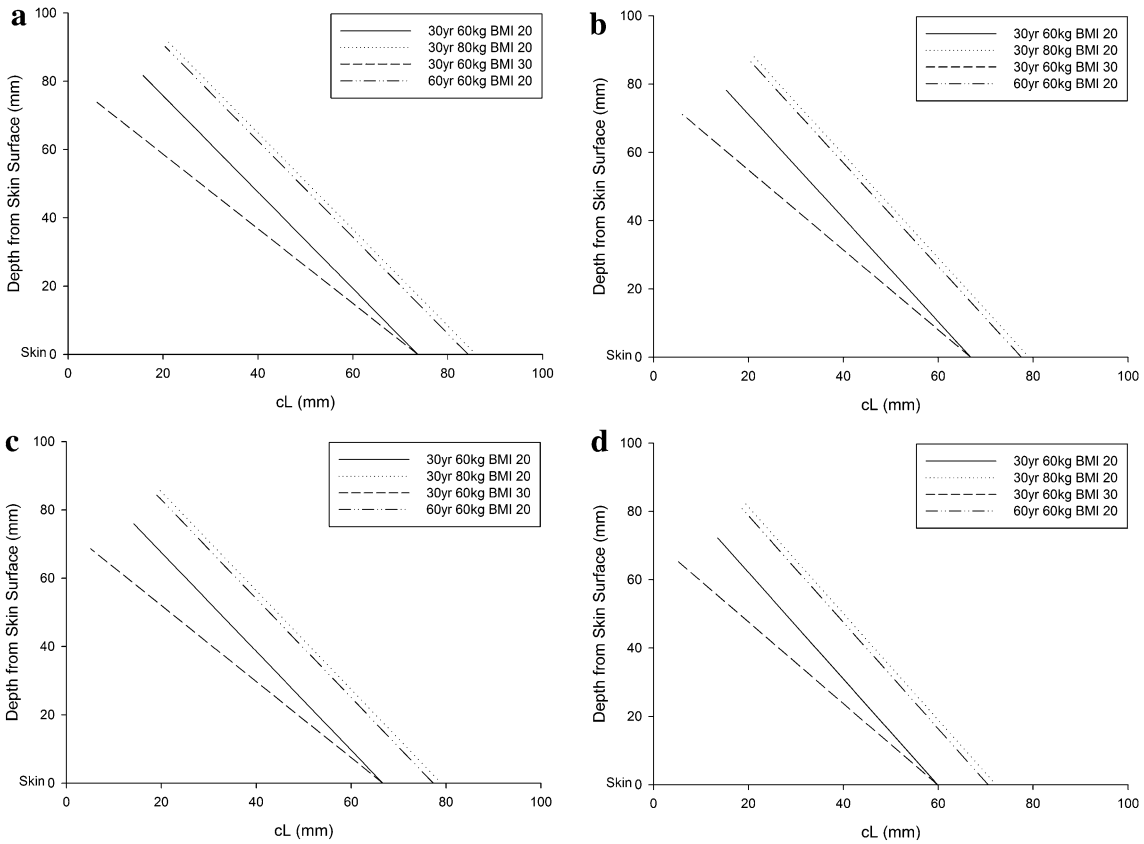

Fig. 3 Schematic trajectories were drawn based on the results of simulation; level T2 for males (**a**) and females (**b**), level T3 for males (**c**) and females (**d**). The *horizontal axis* is the skin surface and the *vertical axis* is the central sagittal line. This simulation does not show recommended trajectory but it shows the most lateral limit trajectory which contacts the parietal pleurae. Lung and parietal pleurae are supposed to be located on the right upper quadrant of the coordinate plane

be considered suitable for lateral limit entering point. The reason for referring to the one-tailed 0.5 % point of inter-individual variability for medial shift is that the percutaneous pneumothorax incidence has been known to be 0.2–0.9 %.

This modeling process was not intended to get rid of the fluoroscopy from the thoracic sympathectomy procedure. The application of the model would rather help a physician determine the lateral limit point and maximum angles that should not be passed over. When applying the results of the models for PTS procedure, the fluoroscope can be rotated obliquely as much as the angle between aM and aL, then, the entry point can be marked on the skin on the way of trajectory with the tunnel vision technique. If the marking point on the skin is located at least 24.3 mm medial to the calculated L point, it would be considered as a safe point.

Measurements of males are generally longer or wider than those of females. However, in the case of angle aM, measurements were wider for females, even though differences between males were small, which might be related to the vertebral body size. The vertebral body width which is the distance between left and right borders and length which is the distance between anterior and posterior borders are shorter in women than in men [14]. A relatively small size of vertebral body would have the target point (lateral side of vertebral body at which thoracic sympathetic ganglion is supposed to be) be located more medially and it might have the aM larger than that for men.

The cL of T2 was longer than that of T3 in males, even though the angle aL did not show significant difference between levels. Accumulation of fatty tissue along the lower cervical and upper thoracic area, known as a hump pad [15], might explain these results. The thicker fatty tissue accumulated on T2 could make the cL longer, even though the aL did not differ between levels. Accumulation of fatty tissue could be a major variability of measurement of this study. BMI is one of the important components for describing aL. Not only the BMI but also patient's other physical constitutions such as chest width would be a good candidate and large influential factor for aL measurements. BMI is closely correlated with chest width [16] so that the aL measurements must have been closely correlated with chest width if the chest width measures were investigated in this study as measurements of interest.

In the current study, age was modeled as an important covariate for cL. Gayzik et al. [17] reported that the variation

of the human rib cage in shape with age is significant in their geometric morphometrics study. They exhibited shape change consistent with the clinical observations in the manner of increasing kyphosis and rounding of the thoracic cage. This feature corresponds to the modeling results of the current study, that is, the cL model included age as a significant covariate. There was a similar previous report by Kim et al. [18], which said that the oblique angle decreases with age, while the current study shows that the angle is related to the BMI. Above all, the beneficial points of the current study against previous similar reports is that the current study makes it possible to predict an individualized safety margin along with the inter-individual variability.

Excessive medial approaches are often blocked by the articular process or the vertebral body itself. The shape and size of the upper level of thoracic vertebral bodies are attributed to the reason why excessive medial approaches cannot reach the target. The size of the upper level of thoracic vertebral bodies is relative small compared to the prominent superior articular process. The lateral side of the vertebral body shape is concave to lateral when it is viewed in a coronal section [14]. The target point of thoracic sympathectomy is usually located in the middle of the lateral concave site, causing the sympathetic ganglion to be located more on the medial side than the articular process or dorsal part of the vertebral body.

For the limitations of this study, even though modeling can reveal the influence of individual characteristics, the models built on the current data set cannot predict a safe window for the person whose weight or age is beyond the upper or lower limits of the current modeling data set. BMI of this study ranges from 18 to 30 (kg/m^2), which does not include a wide range of BMI, therefore the current study model has difficulty in predicting safe windows for the obese person with BMI over 30. The safety window investigated in this study does not guarantee that it could remove all the incidence of pneumothorax. However, the modeling process can help physicians to calculate the safe window and maximum lateral point (cL) from the patients' demographic characteristics and decide where the needle should be inserted.

In conclusion, population analysis of the measurements related to PTS for avoiding pneumothorax could suggest the safe margin and safety window from the result of prediction values calculated from the patients' demographic information and the interindividual variability deduced from the modeling process.

References

1. Ohseto K. Efficacy of thoracic sympathetic ganglion block and prediction of complications: clinical evaluation of the anterior paratracheal and posterior paravertebral approaches in 234 patients. J Anesth. 1992;6:316–31.
2. Straube S, Derry S, Moore RA, Cole P. Cervico-thoracic or lumbar sympathectomy for neuropathic pain and complex regional pain syndrome. Cochrane Database Syst Rev. 2013;9: CD002918.
3. Wilkinson HA. Hand edema after cervical fusion. JAMA. 1983;249:652 (letter).
4. Wilkinson HA. Percutaneous radiofrequency upper thoracic sympathectomy. Neurosurgery. 1996;38:715–25.
5. Hirose M, Tabata M, Sakai M, Takeuchi K. C-arm fluoroscopic cone-beam CT for guidance of chemical thoracic sympathectomy. J Anesth. 2011;25:142–3.
6. Ohseto K. Contrast radiography and effects of thoracic sympathetic ganglion block–anatomical analysis. J Anesth. 1991;5:132–41.
7. Agarwal-Kozlowski K, Lorke DE, Habermann CR, Schulte am Esch J, Beck H. Interventional management of intractable sympathetically mediated pain by computed tomography-guided catheter implantation for block and neuroablation of the thoracic sympathetic chain: technical approach and review of 322 procedures. Anaesthesia. 2011;66:699–708.
8. Dondelinger RF, Kurdziel JC. Percutaneous phenol block of the upper thoracic sympathetic chain with computed tomography guidance. A new technique. Acta Radiol. 1987;28:511–5.
9. Chuang KS, Liu JC. Long-term assessment of percutaneous stereotactic thermocoagulation of upper thoracic ganglionectomy and sympathectomy for palmar and craniofacial hyperhidrosis in 1742 cases. Neurosurgery. 2002;51:963–9 (discussion 969–70).
10. Gibiansky L, Gibiansky E, Bauer R. Comparison of Nonmem 7.2 estimation methods and parallel processing efficiency on a target-mediated drug disposition model. J Pharmacokinet Pharmacodyn. 2012;39:17–35.
11. Jonsson EN, Karlsson MO. Xpose–an S-PLUS based population pharmacokinetic/pharmacodynamic model building aid for NONMEM. Comput Method Progr Biomed. 1999;58:51–64.
12. Brendel K, Dartois C, Comets E, Lemenuel-Diot A, Laveille C, Tranchand B, Girard P, Laffont CM, Mentre F. Are population pharmacokinetic and/or pharmacodynamic models adequately evaluated? A survey of the literature from 2002 to 2004. Clin Pharmacokinet. 2007;46:221–34.
13. Steyerberg EW, Bleeker SE, Moll HA, Grobbee DE, Moons KG. Internal and external validation of predictive models: a simulation study of bias and precision in small samples. J Clin Epidemiol. 2003;56:441–7.
14. Masharawi Y, Salame K, Mirovsky Y, Peleg S, Dar G, Steinberg N, Hershkovitz I. Vertebral body shape variation in the thoracic and lumbar spine: characterization of its asymmetry and wedging. Clin Anat. 2008;21:46–54.
15. Aldrete JA, Mushin AU, Zapata JC, Ghaly R. Skin to cervical epidural space distances as read from magnetic resonance imaging films: consideration of the "hump pad.". J Clin Anesth. 1998;10:309–13.
16. Henneberg M, Ulijaszek SJ. Body frame dimensions are related to obesity and fatness: lean trunk size, skinfolds, and body mass index. Am J Hum Biol. 2010;22:83–91.
17. Gayzik FS, Yu MM, Danelson KA, Slice DE, Stitzel JD. Quantification of age-related shape change of the human rib cage through geometric morphometrics. J Biomech. 2008;41:1545–54.
18. Kim WH, Lee CJ, Kim TH, Shin BS, Sim WS. The optimal oblique angle of fluoroscope for thoracic sympathetic ganglion block. Clin Auton Res. 2011;21:89–96.